ELSEVIER

Journal of Photochemistry and Photobiology B: Biology 38 (1997) 258–268

Journal of PHOTOCHEMISTRY AND PHOTOBIOLOGY B:BIOLOGY

PDT light dosimetry revisited

Leonard I. Grossweiner *

Wenske Laser Center, Ravenswood Hospital Medical Center, 4550 N. Winchester Ave., Chicago, IL 60640, USA

Received 24 July 1996; revised 7 October 1996; accepted 16 October 1996

Abstract

A versatile PDT light dosimetry model is described incorporating the effects of drug photobleaching, drug elimination, and normal tissue damage. The dependence of the necrosis depth (d_n) on the incident light dose for the four major modes of PDT light delivery has the form: $d_n = \delta \log_e(DG)$, where δ is the optical penetration depth of the tumor tissue, D is the ratio of the incident light dose to the energy fluence at the necrosis threshold, and G is a function of the tissue optical constants. Light dosimetry graphs were calculated for Photofrin® at standard conditions.

Keywords: Photodynamic therapy; Light dosimetry; Photofrin®

1. Introduction

The photodynamic therapy (PDT) drug Photofrin® (PF) has received recent regulatory approvals for treatment of specific malignancies. The clinical trials leading to approvals were performed according to protocols designed to provide statistical data. The optimization of PDT treatment planning is highly desirable with the ongoing transition of PDT from an experimental to a fully approved therapy, Treatment planning based on the clinical literature requires simple radiometry calculations. This procedure may achieve statistical responses comparable to clinical trials. However, the protocols employed for clinical trials do not consider important factors relevant to the PDT response, especially the tumor dimensions and optical properties. Analytical light dosimetry modeling is an alternative approach. The present methodology involves assumptions about the PDT action mechanism and light propagation in tumor tissues. The objective is to calculate the delivered light dose which ensures that necrosis is achieved in all tumor regions. There is a considerable literature on light dosimetry models for PDT [1–15]. The present and prior models are based on the assumption that PDT is a "threshold" process, in which a minimum energy density must be absorbed by the localized photosensitizer in order to initiate tumor necrosis. The complex rate kinetics associated with a threshold process may be circumvented by relating the necrosis depth (d_n) to the incident light dose. Treatment planning then involves matching the calculated necrosis depth to the tumor dimensions. The present model incorporates features of the earlier work as well as new results. The analysis based on the diffusion approximation leads to dosimetry relations having the same form for four principal modes of PDT light delivery. The numerical results for front surface light delivery are in good agreement with more accurate calculations based on Monte Carlo modeling. Dosimetry results are presented in graphical form for PF.

Abbreviations: a, radius of spherical or cylindrical cavity; BCC, basal cell carcinoma; C_{so}, localized photosensitizer concentration; CI, cylindrical insertion (delivery); CS cylindrical surface (delivery); d_n, necrosis depth; d_n^*, maximum necrosis depth for negligible normal tissue damage; $E_0 t$, incident irradiance; F, magnitude of energy flow vector; FS, front surface (delivery); g, average cosine of single-particle scattering angle; K_s, specific photobleaching rate constant; M, M', refractive index mismatch correction factors; PF, Photofrin ®; PS, point surface (delivery); q^*, energy fluence at necrosis threshold; R_d, diffuse reflection coefficient; R_{sp}, specular reflection coefficient; r_i, internal reflection coefficient for diffuse light; SCC, squamous cell carcinoma; T, drug elimination halflife; W_s^*, energy density absorbed by photosensitizer at necrosis threshold; α, photon diffusion constant; β, drug elimination rate constant; β', ratio of total light fluence to direct (non-scattered) fluence for PS delivery; δ, optical penetration depth; φ, energy fluence rate; τ_s, specific absorption coefficient of photosensitizer; Γ, drug dose–light dose non-reciprocity factor; μ_a, linear absorption coefficient; μ_s, linear scattering coefficient

* Corresponding author. Tel: + 1 773 878-4300, ext. 2553; fax: + 1 773 878-2649; email: lgflash@aol.com

PII S1011-1344(96)07469-6

2. Photophysical and photochemical basis of the model

The major determinants of the threshold dose are combined in an energy fluence parameter q^* (J m^{-2}) which depends on the type and concentration of the PDT drug, the treatment

wavelength, and the intrinsic photosensitivity of the tumor. Ideally, q^* does not depend on the tumor optical properties, its dimensions, and the mode of light delivery. It is convenient to derive the dosimetry relations by ignoring drug photobleaching and pharmocokinetics and then evaluate their effects on the calculated values of d_n. The basic photochemical quantity in the present model is the minimum energy density W_s^* (J m^{-3}) that must be absorbed by the localized photosensitizer in order to initiate tumor necrosis. This quantity is related to q^* according to:

$$W_s^* = \tau_s C_{so} q^* \quad (1)$$

where C_{so} (μg g^{-1}) is the localized drug concentration and τ_s (cm^{-1} μg^{-1} g) is the specific absorption coefficient of the photosensitizer per unit concentration. The necrosis condition may be expressed as:

$$\varphi(r_n)t = q^* \quad (2)$$

where $\varphi(r_n)$ (W m^{-2}) is the energy fluence rate at a tissue location r_n where the necrosis threshold is just attained and t (s) is the treatment time. Four modes of PDT light delivery are considered: *front surface* (FS)—a uniform irradiance incident beam delivered by an external source; *point surface* (PS)—an isotropic source centered in a spherical cavity; *cylindrical surface* (CS)—a line source centered in a cylindrical lumen; *cylindrical insertion* (CI)—a line source embedded in the tumor tissue. The functions $\varphi(r)$ were derived in prior work based on the photon diffusion approximation [12]. Substituting $\varphi(r)$ in Eq. (2) leads to the dependence of d_n on the incident light dose (Appendix A). The result for FS delivery is:

$$d_n = \delta \log_e(ME_o t/q^*) \quad (3)$$

where $(E_o t)$ is the incident fluence and the dimensionless constant M is given by Eq. (A4). The value of M depends on the tumor optical constants and the mismatch between the tissue refractive index (n) and the external medium. The results for the four geometries have the form:

$$d_n = \delta \log_e(DG) \quad (4)$$

where d_n is the necrosis depth measured from the illuminated tissue surface, D is the incident fluence scaled to q^*, and function G depends on the optical constants (Table 1).

Table 1
Necrosis depth calculation for different modes of light delivery

Light delivery mode	$d_n = \delta \log_e(DG)$	
	D	G
Front surface (FS) [a]	$ME_o t/q^*$	1
Point surface (PS) [b]	$P_o tM'/\pi a^2 q^*$	$\frac{a}{a+d_n}\frac{1}{1+2\alpha/a+2\alpha/\delta}$
Cylindrical surface (CS)	$2P_o tM'/\pi Laq^*$	$\frac{1}{1+2\alpha/\delta}\sqrt{a(a+d_n)}$
Cylindrical insertion (CI)	$P_o t/L\alpha q^*$	$\sqrt{\delta/2\pi d_n}$

[a] M is given by Eq. (A4).
[b] $M' = \frac{1}{4}(1+2\alpha/\delta)M$.

Table 2
Calculated values of R_d and δ for some in vitro human tissues at 630–635 nm

Tissue	R_d [a]	δ (mm) [b]	Ref.
Aorta	0.59	1.2	[30]
Bladder [c]	0.52	2.5	[18]
Brain			
(white matter)	0.08	2.4	[31]
(gray matter)	0.14	1.1	[31]
Breast	0.60	3.2	[32]
Dermis	0.33	0.6	[33]
Epidermis	0.35	0.9	[34]
Liver	0.23	0.7	[35]
Lung	0.29	0.2	[32]
Uterus	0.77	0.9	[32]

[a] Calculated with Eq. (A5) from published optical constants.
[b] Calculated with Eq. (A2) from published optical constants.
[c] 650 nm.

3. Light dosimetry calculations

3.1. Light dosimetry for PF at standard conditions

Standard conditions for PF are taken as 630 nm irradiation and 2.0 mg kg^{-1} injection dose with a post-injection time delay of 24–48 h.

3.1.1. Estimation of parameters

The key parameters in Eq. (4) are δ and q^*. δ can be measured directly or calculated from the tissue optical constants using Eq. (A2). Typical values of δ for non-pigmented tissues range from 1–3 mm for red and near-infrared light [16]. The value $q^* = 39$ J cm^{-2} was calculated for PF at standard conditions from clinical data indicating that PDT of basal cell carcinoma (BCC) required a minimum $(E_o t) \approx 20$ J cm^{-2} [17]. The parameter M depends on the diffuse reflection coefficient (R_d) of the tissue. Some values of δ and R_d for red light calculated from published optical constants are given in Table 2. The calculated values of d_n are insensitive to the numerical values of the quantities inside the logarithmic terms. The present calculations are based on $n = 1.38$ and $\alpha = 0.05$ cm (see Appendix A).

3.1.2. Front surface delivery

FS delivery is used for PDT of superficial tumors with an external optical fiber and for "focal" light delivery to interstitial tissue surfaces. The dependence of the scaled necrosis depth d_n/δ on the incident light dose (E_ot) is graphed in Fig. 1. The leveling of d_n cannot be offset by using an arbitrarily high light dose without undue tissue heating. A "rule of thumb" maximum for E_o is 150 mW cm^{-2} for PF at standard conditions. Assuming $\delta = 2$ mm and $R_d = 0.3$ for a typ-

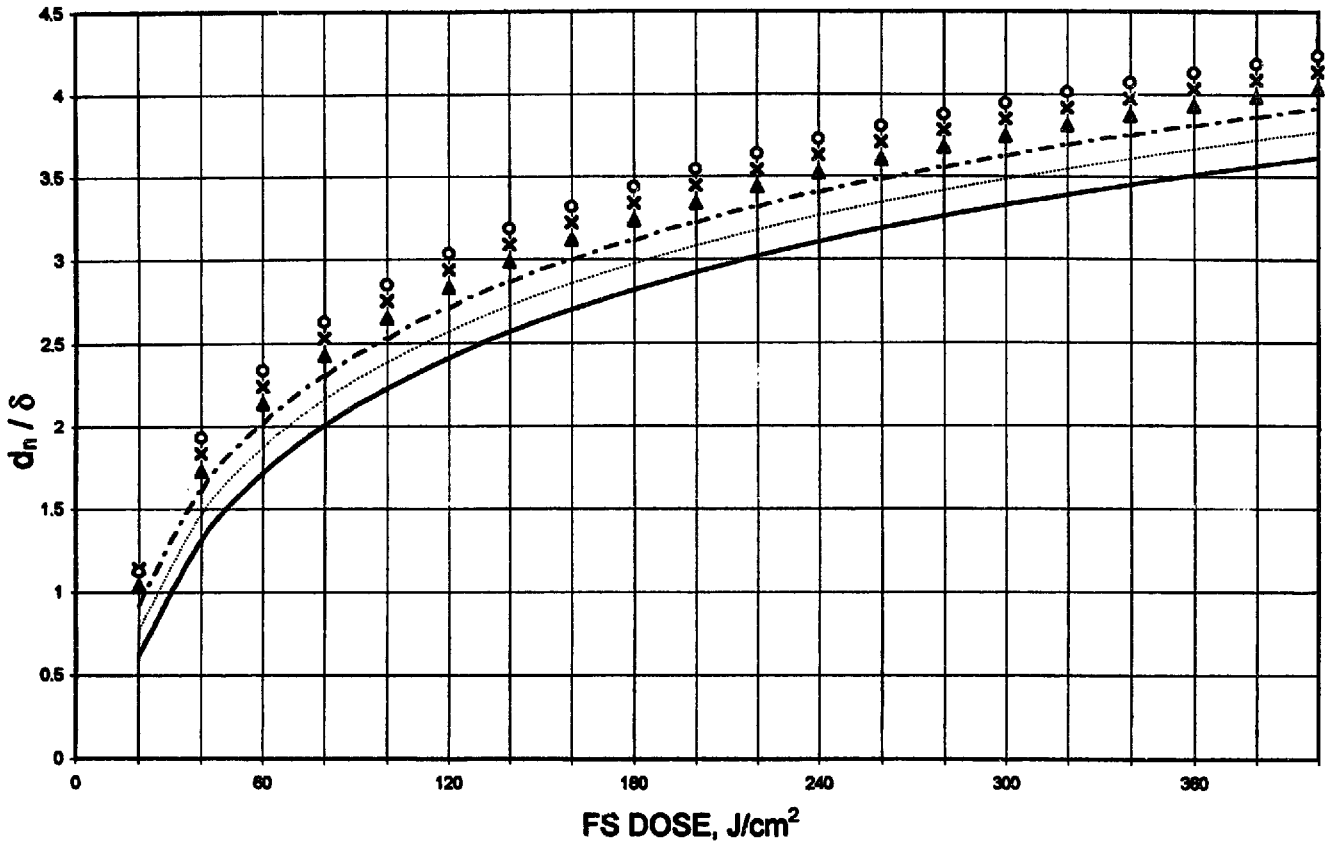

Fig. 1. Front surface light delivery with PF at standard conditions. Dependence of scaled necrosis depth (d_n/δ) on FS dose and diffuse reflectivity (R_n): ——— $R_n = 0.1$; · · · $R_n = 0.2$; – · – $R_n = 0.3$; ▲ $R_n = 0.4$; x $R_n = 0.5$; ∘ $R_n = 0.6$.

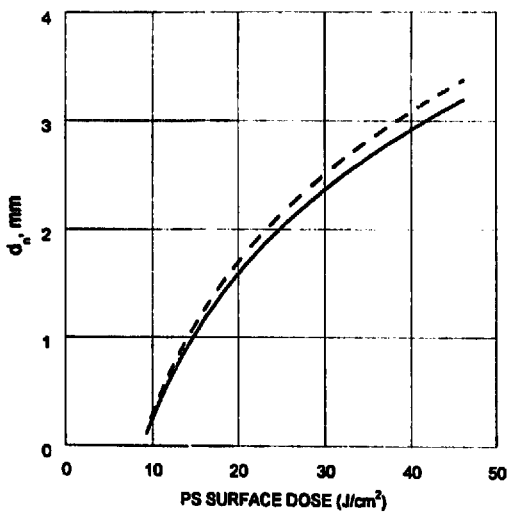

Fig. 2. Point surface light delivery with PF at standard conditions. Dependence of d_n on the total surface dose including scattered light. The assumed cavity volume is 300 cm³ and $\delta = 2.0$ mm: solid line, calculated for PS delivery; dashed line, calculated for FS delivery.

ical non-pigmented tumor leads to maximum effective $d_n \approx 7$ mm for FS delivery.

3.1.3. Point surface delivery

PS delivery is employed for PDT of the urinary bladder. Typical values of the cavity radius a, about 2–4 cm, are much larger than α and δ and, therefore, calculations of d_n based on Eq. (4) for PS delivery are close to Eq. (3) at the equivalent surface dose. The values of d_n are compared in Fig. 2 for a 300 cm³ cavity volume and $\delta = 2$ mm. The good agreement indicates that the FS calculation may be employed for PS delivery with $(E_0 t) = P_0 t/4\pi a^2$. The "integrating sphere" effect is a complication for PS light delivery. Scattered light reflected by the bladder wall may increase the effective fluence by a factor of β' which is strongly dependent on the patient [18]. A typical value $\beta' = 5$ would increase d_n by an additive factor of 1.6δ. In situ light dosimetry measurements are highly desirable for bladder PDT to determine the true light dose.

3.1.4. Cylindrical surface delivery

CS delivery is used for PDT within cylindrical cavities, including the esophagus, bronchus, and vaginal wall. For a given light dose, d_n depends on the lumen diameter $2a$, R_d, and δ. Fig. 3(a) shows the dependence of d_n on light dose and R_d for $2a = 25$ mm and $\delta = 2.0$ mm. Fig. 3(b) shows the dependence of d_n on $2a$ for $R_d = 0.25$ and $\delta = 2.0$ mm Fig. 3(c) shows the dependence of d_n on δ for $R_d = 0.25$ and $2a = 25$ mm. The equivalent surface dose calculation is useful only for large a.

3.1.5. Cylindrical insertion delivery

CI delivery is employed for PDT of bulky tumors. The dependence of the necrosis radius r_n on the CI dose is plotted in Fig. 4. The maximum effective necrosis diameter ($2r_n$) is

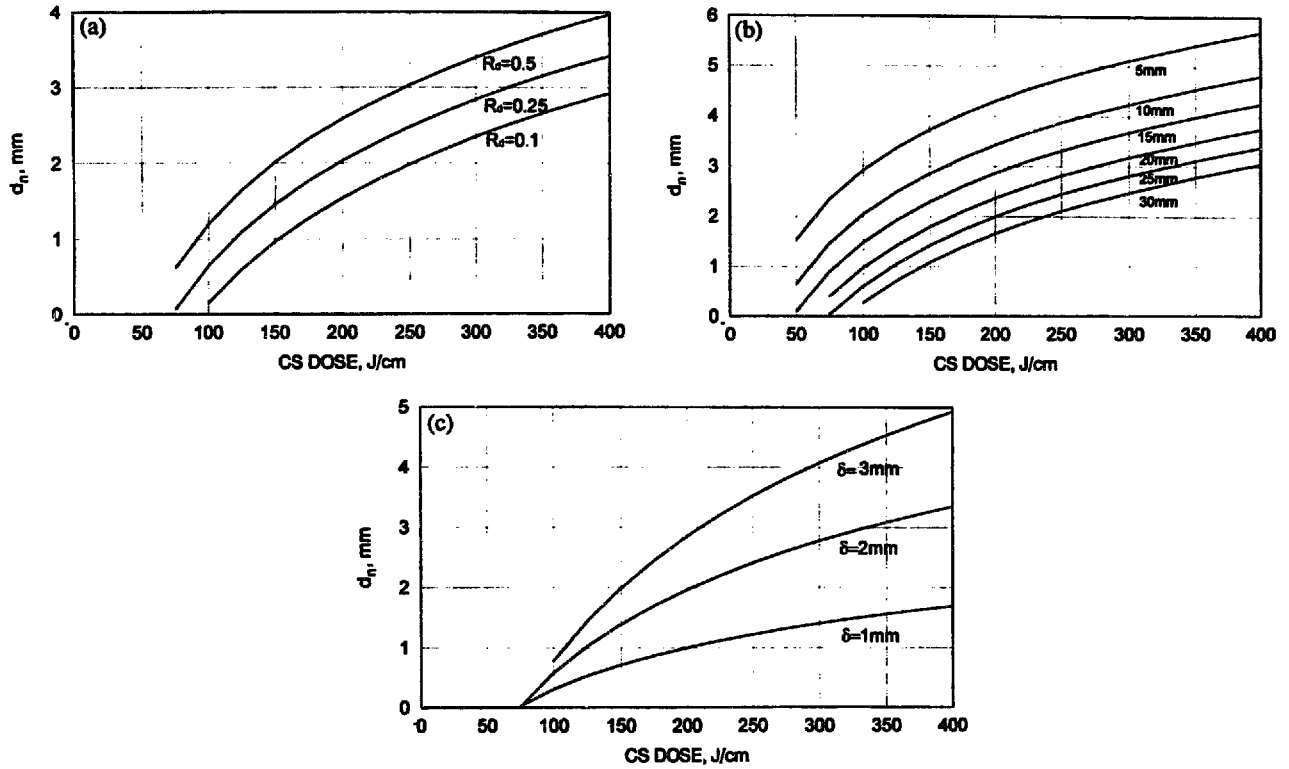

Fig. 3. Cylindrical surface light delivery with PF at standard conditions. Dependence of d_n on CS dose. (a) For assumed 25 mm diameter, $\delta = 2.0$ mm, and different R_n. (b) For assumed $R_n = 0.25$, $\delta = 2.0$ mm, and different lumen diameters. (c) For assumed $R_n = 0.25$, 25 mm lumen diameter, and different δ.

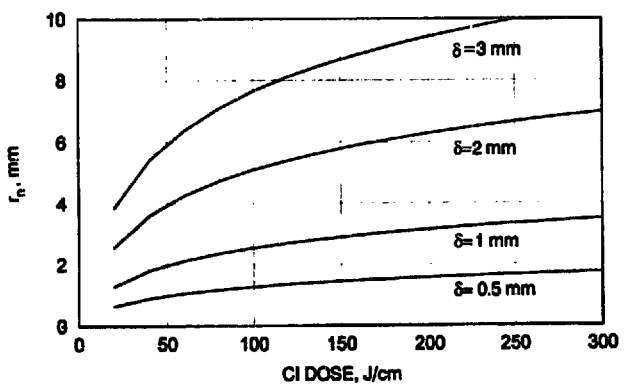

Fig. 4. Cylindrical insertion light delivery with PF at standard conditions. Dependence of necrosis radius (r_n) on CI dose at different δ.

about 12 mm for $\delta = 2$ mm. CI delivery cannot be approximated by a surface dose calculation.

3.2. Generalized light dosimetry

Fig. 5 shows generalized light dosimetry plots for FS delivery with the incident light dose scaled to q^* and the necrosis depth scaled to δ. The results were calculated with the more accurate Eq. (A6) and the parameters in Ref. [19]. The normalized curves are insensitive to R_d, which simplifies the applications to different tumors. Fig. 5 should be applicable for any PDT drug that functions via the threshold mechanism.

4. Effects of drug photobleaching and elimination

The light dose and PF dose are not "reciprocal" quantities, e.g. halving the PF dose requires more than twice the light dose to achieve equivalent necrosis. This effect is attributed to photobleaching of PF by the PDT light [1,2,12,13]. Other consequences of photobleaching are an upper bound on d_n and sparing of those normal tissues having low initial drug concentrations. Photolysis of PF in vitro generates a photosensitizing "red" photoproduct which was not considered [20]. Elimination refers to a decrease of the localized drug concentration during the PDT procedure. This effect may be a consequence of the pharmacokinetics or light-induced changes in the tumor properties. In either case, the rate of elimination is specified by an effective halftime T. The detailed analysis is given in Appendix B.

The photobleaching rate constant (K_s) is defined as the fractional loss of active photosensitizer per unit energy density absorbed by the active photosensitizer. $K_s = 2.54\ \mu g\ g^{-1}\ J^{-1}\ cm^3$ was calculated from clinical results indicating that PDT of BCC with PF requires about 30 J cm^{-2} at standard conditions (2.0 mg kg^{-1}) and about 200 J cm^{-2} at 1.0 mg kg^{-1} [21]. The corresponding rate constant in terms of the incident fluence is 0.025 J^{-1} cm^2. An experimental result for human patients based on loss of in vivo PF fluorescence is 0.040 J^{-1} cm^2 [2]. Drug dose–light dose non-reciprocity is significant for PF. The calculations in Table 3 based on Eq. (B6) assume that C_{so} is proportional to

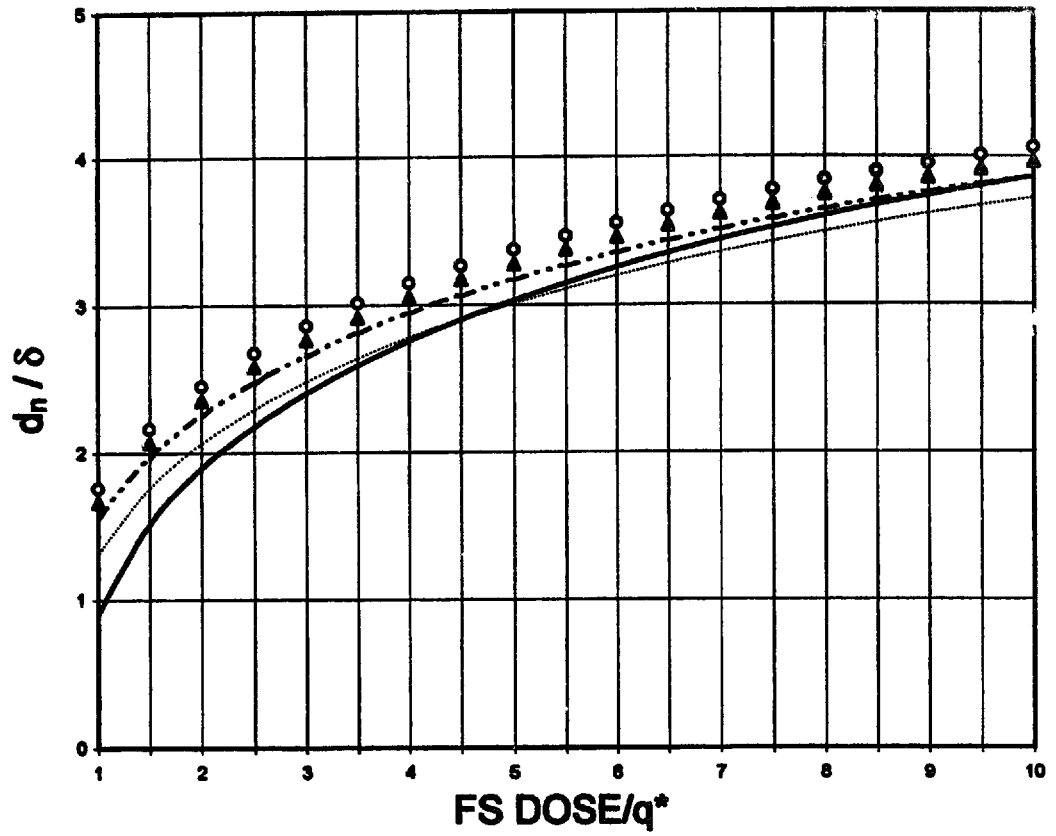

Fig. 5. Generalized front surface light dosimetry. Dependence of d_n/δ on $(E_o t)/q^*$ for: ——— $R_n = 0.1$; · · · $R_n = 0.2$; – · – $R_n = 0.3$; ▲ $R_n = 0.4$; x $R_n = 0.5$; ○ $R_n = 0.6$. Based on Eq. (A6).

Table 3
Effects of photobleaching and elimination on PDT light dosimetry

PF dose (mg kg^{-1})	$E_o t$ (rel)	Γ [b]
A. Effect of photobleaching on light dose [a]		
2.0	1	1
1.75	1.22	1.07
1.5	1.58	1.19
1.25	2.30	1.44
1.0	6.67	3.33

B. Effect of photobleaching on necrosis depth [a]

$d_n' = d_n - 0.32\delta$

C. Effect of drug elimination on necrosis depth [c]

$$d_n' = d_n - \delta \log_e\left(\frac{1-0.693/T}{0.693/T}\right)$$

[a] For PF at standard conditions.
[b] Drug dose × light dose.
[c] For a photosensitizer having elimination half-life T.

the injection dose. The "non-reciprocity factor" Γ is the product of the relative drug dose and light dose. Γ depends only on the clinical results used to evaluate K_s and not its numerical value. Photobleaching leads to an upper limit in the necrosis depth that depends on the initial localized drug concentration. For PF at standard conditions photobleaching reduces d_n by 0.32δ at any light dose.

4.1. Effects of photobleaching and drug elimination on necrosis depth

For elimination without photobleaching d_n is reduced by: $\delta \log_e[(1-\beta)/\beta]$, e.g. d_n is smaller by 0.63δ for $T = 2$ h. A more complicated relation obtains when photobleaching and elimination take place. Fig. 6 shows some numerical calculations of d_n/δ based on Eq. (B9) for a hypothetical short-lived photosensitizer having the same q^* and K_s as PF and $E_o = 150$ mW cm^{-2}. The dashed line is the limiting value PF at standard conditions ignoring photobleaching and elimination. The practical effect of photobleaching and elimination on d_n is relatively small. According to Fig. 6, $d_n = 2.73\delta$ for a 1 h halflife and a 20 min irradiation (180 J cm^{-2}). The same light dose for PF leads to $d_n = 3.20\delta$ without photobleaching and $d_n = 2.88\delta$ with the photobleaching correction.

4.2. Normal tissue damage

Photochemical damage to normal tissues sets an upper limit on the PDT light dose. A practical relation is derived by calculating the maximum necrosis depth in the tumor without inducing necrosis of normal tissues receiving the same light dose (d_n^*). The result based on Eqs. (1) and (3) assuming the same W_s^* for normal and malignant tissues and setting $d_n = 0$ in the normal tissue leads to:

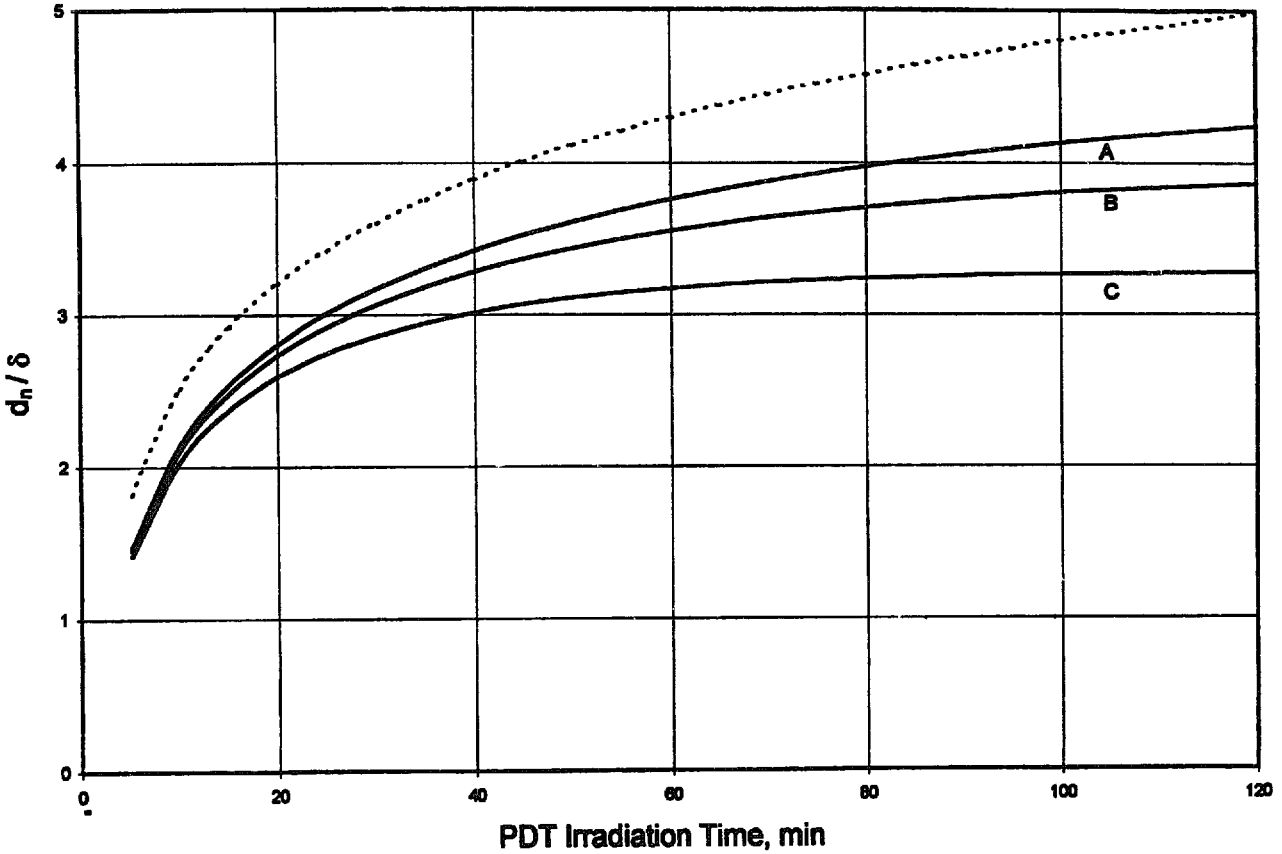

Fig. 6. Effect of photobleaching and drug elimination on scaled necrosis depth (d_n/δ) on irradiation time and elimination halflife (T) for a short-lived drug with the same photosensitizing and photobleaching properties as PF. The incident irradiance is $E_o = 150$ mW cm^{-2}. (A) $T = 2.0$ h; (B) $T = 1.0$ h; (C) $T = 0.5$ h. The dashed line applies for PF at standard conditions without photobleaching and elimination.

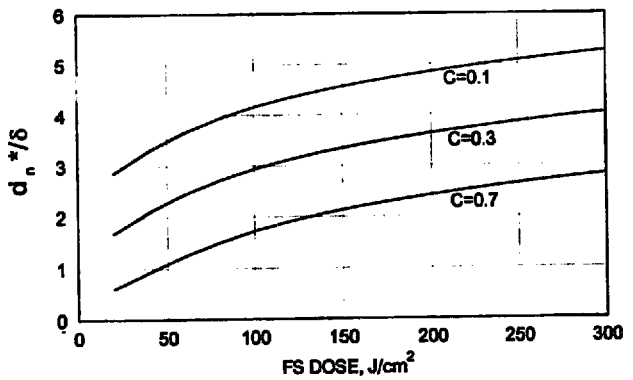

Fig. 7. Maximum scaled necrosis depth (d_n^*/δ) leading to neglible normal tissue damage for PF at standard conditions. C is ratio of the drug concentration in normal tissue to that in the tumor.

$$d_n^*/\delta = \log_e(C_{so}/C_{so}') \quad (5)$$

where C_{so}' and C_{so} are the drug concentrations in the normal tissue and the tumor, respectively. The concentration ratio $C \equiv C_{so}'/C_{so}$ is equivalent to the "therapeutic ratio" for PDT because the light dose leading to necrosis depends on the localized drug concentration. According to Eq. (5), $d_n^* = 1.2\delta$ for $C_{so}'/C_{so} = 0.3$. The small maximum value of d_n^* ignores photobleaching which is significant at the low PF drug concentrations localized in normal tissues. The equivalent calculation including photobleaching leads to Eq. (B10), where it is assumed that the tumor and normal tissues are exposed to the same fluence. d_n^* depends on the light dose because the normal and tumor tissues have different and changing drug concentration profiles during the course of the irradiation. Plots of d_n^*/δ are given in Fig. 7 for PF at standard conditions, $R_d = 0.37$, and different values of C, e.g., $C = 0.3$ gives $d_n^* = 1.90\delta$ at 30 J cm^{-2} and 3.34δ at 150 J cm^{-2}. The corresponding values of d_n^* calculated with Eq. (3) and corrected for photobleaching are 1.09δ and 2.69δ. Thus, the predicted d_n for these conditions are lower than the corresponding d_n^*, which illustrates that photobleaching spares normal tissues having low initial PF concentrations.

5. Summary of model results

The present light dosimetry model leads to the following general conclusions:

1. The calculated necrosis depth levels off at high light dose for FS and CI delivery. The practical upper limits on d_n for $\delta = 2$ mm and PF at standard conditions are ≈ 7 mm for FS delivery (Fig. 1) and ≈ 12 mm ($2r_n$) for CI delivery (Fig. 4).
2. For a scaled light dose ($E_o t$)/q^*, the scaled necrosis depth d_n/δ has a weak dependence on R_d (Fig. 5).

Table 4
Application of model results to hypothetical PDT procedures [a]

Cancer	Light dose	Delivery mode	Assumed parameters			Calculated d_n (mm)
			Dimensions	R_d	δ (mm)	
T_a bladder cancer	15 J cm^{-2} [b]	PS	300 cm^3	0.5	2.5	2.1
Head and neck SCC	125 J cm^{-2}	FS		0.25	2.0	5.4
	75 J cm^{-1}	CI		0.25	2.0	9.2 [c]
Skin BCC	30 J cm^{-2}	FS		0.37	1.0	1.4
Barrett's dysplasia	250 J cm^{-1}	CS	25 mm dia	0.25	2.0	2.5
Obstructing esophageal cancer	300 J cm^{-1}	CS	5 mm dia	0.25	2.0	5.3

[a] For PF at standard conditions.
[b] Direct plus scattered fluence.
[c] Diameter of necrotic region.

3. Photobleaching of PF leads to significant "non-reciprocity" between light dose and drug dose (Table 2).
4. Photobleaching and elimination for PF at standard conditions may have a significant effect on d_n (Fig. 6).
5. Photobleaching of PF protects those normal tissues having low initial drug concentrations (Fig. 7).

6. Discussion

A realistic evaluation of the accuracy is a key issue for modeling of PDT light dosimetry. The present model represents a compromise between theoretical complexity and computational convenience. The numerical values of the principal drug-related variables, q^* and K_s, were estimated from clinical data for BCC. Whether the same values are applicable for other tumors requires further evaluation. δ is most important tissue-related variable owing to the linear dependence of d_n on δ. Judicious guessing of δ is not impractical, although this approach cannot be expected to optimize a procedure. In vitro determinations of δ are subject to sample variability and do not account for light absorption by blood [22]. Light absorption by the PDT drug also should reduce δ. However, a much larger effect was found for an animal model, in which administration of PF led to a large increase of $\mu_s(1-g)$ in excised tumor tissues [23]. A similar effect of PF on tumor optical constants was deduced from skin reflection measurements on patients treated for basal cell nevus syndrome. At 24 h after administration of PF, the skin reflectivity was slightly lower in uninvolved skin, but it was *higher* in basal cell cancer (BCC) sites [24,25]. This result can only be explained by an enhancing effect of PF on light scattering in the BCC. The most reliable values of δ for PDT modeling would be obtained from in vivo measurements immediately prior to PDT.

The present model treats the rate-controlling step in PDT as equivalent to a photochemical process. The threshold calculation implies that PF is localized in tumor tissues. More hydrophilic PDT drugs with shorter plasma lifetimes may remain in the circulation. This case can be accommodated in the model by employing an appropriate value of q^*. Depletion of tumor oxygen is not included in the present model. Clinical data showing that satisfactory results can be achieved for a wide range of treatment variables suggest that oxygen depletion is not a crucial factor for PF at standard condition [17]. Other factors that may affect tumor photosensitivity are tissue heating induced by the PDT light and adjuvant drugs. These effects can be included in the model by adjusting the value of q^*.

There is no definitive method for evaluating the accuracy of model predictions. Table 4 gives some calculated values of d_n for hypothetical PDT procedures. The result for superficial (T_a) bladder cancer is based on the surface dose used in Phase III clinical trials. The calculated $d_n \approx 2$ mm predicts that necrosis is limited to superficial lesions. Bulky head and neck squamous cell cancers (SCC) were successfully treated by the combination of FS and CI delivery using modeling as a guide to the light dosimetry, [8,26]. BCC are typically treated at 20–40 J cm^{-2} for PF at standard conditions. The predicted d_n extends into the upper dermis. A CS light dose of 250 J cm^{-1} as might be used for PDT of Barrett's dysplasia leads to $d_n = 2.5$ mm for a 25 mm diameter esophagus. For obstructing esophageal cancer, 300 J cm^{-2} based on Phase III clinical trials predicts a significant reduction of the tumor mass. In general, the model predictions are consistent with estimates of the required necrosis depth for these procedures. It is important to emphasize that modeling is based on idealized conditions and estimated average parameters. Owing to the variability of drug pharmacokinetics, tumor optical properties, and tumor photosensitivity, the model predictions should be used only as a general guide to treatment planning in conjunction with diagnosis and clinical judgment.

Acknowledgements

The author is indebted to Dr Mehmet D. Bilgin and Mr James M. Fernandez for helpful suggestions. Research support by a gift from the Elizabeth S. Boughton Charitable Trust is gratefully acknowledged.

Appendix A. Diffusion model calculations of necrosis depth without drug photobleaching and elimination

The diffusion equation for a uniform medium is

$$\nabla^2\varphi(r) - (\mu_a/\alpha)\varphi(r) = -S(r)/\alpha \quad \text{(A1)}$$

where $\alpha = (1/3)[\mu_a + \mu_s(1-g)]$ is the photon diffusion constant; μ_a is the linear absorption coefficient, μ_s is the linear scattering coefficient, and g is the mean cosine of the single-particle scattering angle. The exact form of the source function $S(r)$ in Eq. (A1) depends on the angular scattering distribution or phase function. The optical penetration depth δ is the distance within the tissue in which the fluence rate is attenuated by e^{-1}. The value of δ in tissue locations distant from sources is given by:

$$\delta = \sqrt{\alpha/\mu_a} \quad \text{(A2)}$$

A.1. Necrosis depth calculations

FS light delivery is modeled by assuming a wide, uniform irradiance light beam incident on a uniform semi-infinite layer. Eq. (A3) is the solution for the "P0-delta" phase function, consisting of an isotropic component plus a solid-angle delta function in the forward direction, and the approximations: $z \gg \alpha$ and $[\mu_a/\mu_s(1-g)]^2 \ll 1$:

$$\varphi(z) = ME_o \exp(-z/\delta) \quad \text{(A3)}$$

where E_o is the incident irradiance and z is the depth into the tissue [12]. The constant M for this approximation is given by

$$M = 3[1 + (2/3)bR_d] \quad \text{(A4)}$$

where R_d is the diffuse reflection coefficient, $b \equiv (r_i + 1)/(r_i - 1)$, and r_i is the internal reflection coefficient at the interface. $r_i = 0.514$ for a typical tissue with n = 1.38. Values of R_d for other tissues may be estimated from the optical constants. The "P0-delta" phase function leads to the following expression:

$$R_d = \frac{N'}{[(1+N') + \sqrt{3}(1+N')][1 + 2b/\sqrt{3}(1+N')]} \quad \text{(A5)}$$

where $N' \equiv \mu_s(1-g)/\mu_a$ [12,27]. Eq. (A5) is exact within the limitations of the diffusion approximation.

A more accurate expression for $\varphi(z)$ close to the interface has the form:

$$\varphi(z) = E_o[C_1 \exp(-k_1 z/\delta) - C_2 \exp(-k_2 z/\delta)] \quad \text{(A6)}$$

Semi-empirical expressions were derived for the dependence of C_1, C_2, k_1, and k_2 on R_d by fitting Eq. (A6) to Monte Carlo calculations for uniform, illuminated semi-infinite layers having $n = 1.38$ and $g = 0.7$–0.9 [19]. The values of C_1 are close to M, e.g. for $R_d = 0.3$, Eq. (A4) gives $M = 4.87$ compared with $C_1 = 4.72$. Eq. (3) for FS delivery is compared to Eq. (A6) for PF at standard conditions and $(E_o t) = 50$ J cm^{-2} in Fig. 8. The good agreement supports the use of the more convenient diffusion approximation.

The light dosimetry expressions for the other modes were derived by setting $S(r) = 0$ and employing the approximate boundary condition:

$$\varphi(a) = 4E(a) - 2F(a) \quad \text{(A7)}$$

where $F(a)$ is the magnitude of diffuse energy flow vector and a is the coordinate at the boundary at which light enters the tissue [28]. The resultant solutions for $\varphi(r)$ are given in Ref. [12]. The light dosimetry relations were calculated by substituting the expressions for φ in Eq. (2) and solving for the necrosis depth leading to Eq. (A8) (same as Eq. (4)):

$$d_n = \delta \log_e(DG) \quad \text{(A8)}$$

where d_n is the necrosis depth measured from the illuminated tissue surface. The functions D and G are given in Table 1. The factor $M' = (1/4)(1 + 2\alpha/\delta)M$ is an approximate correction for refractive index mismatch at the air–tissue interface derived by equating d_n at large a to the results for FS delivery. The present M′ differs from the less accurate M′ in Ref. [12]. Applications of Eq. (A8) for PS delivery should use the total fluence consisting of the direct and scattered light.

q^* for PF at standard conditions was calculated from clinical data showing that PDT of BCC required a minimum $(E_o t) \approx 20$ J cm^{-2} [17]. Setting $d_n \approx \delta$ in Eq. (3) for superficial tumors and taking $M = 5.3$ for BCC at 630 nm leads to $q^* = 39$ J cm^{-2}. The value of M was calculated with Eq. (A4) for $n = 1.38$ and $R_d = 0.37$ for BCC at 630 nm [24]. The values of R_d in Table 2 were calculated with Eq. (A5) using the same optical constants leading to δ. The calculated d_n are insensitive to the parameters in the logarithmic terms. A 25% error in q^* changes d_n by 0.25δ. α does not vary widely for non-pigmented tissues at a given wavelength. The approximate value $\alpha = 0.05$ cm was used for all calculations [1]. A 25% error in α changes d_n by 0.3δ for CI delivery, which is the most sensitive case.

Appendix B. Effect of drug photobleaching and elimination

B.1. Photobleaching model

It is assumed that photobleaching obeys overall first-order photochemical kinetics with rate constant K_s. This mechanism does not apply for a self-photosensitization, e.g. photo-oxidation of the sensitizer mediated by singlet oxygen generated by the sensitizer. In this case, K_s is considered as an empirical rate parameter applicable for the specific conditions. The dependence of the localized drug concentration on the absorbed energy density is given by:

$$-\partial C_s(r,t)/\partial t = K_s[dW_s(r,t)/dt] \quad \text{(B1)}$$

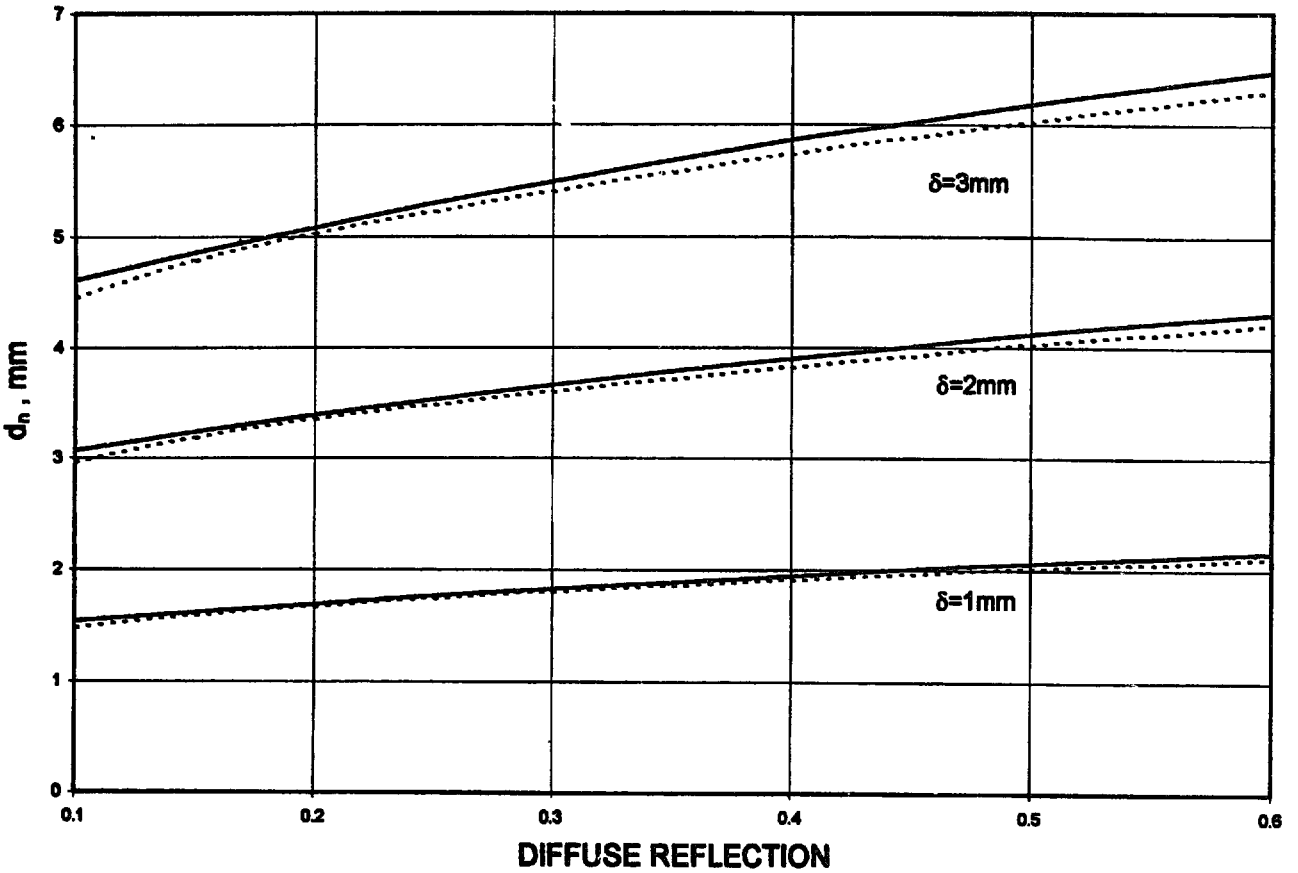

Fig. 8. Front surface light delivery with PF at standard conditions. Dependence of d_n on δ and R_n at 50 J cm^{-2} light dose: solid lines, diffusion approximation; dashed lines, Monte Carlo modeling based on Eq. (A6).

where K_s (μg ml^{-1} J^{-1} cm^3) is the specific photobleaching rate constant per unit absorbed energy density. The effect of photobleaching on the rate of light absorption is given by

$$-\partial W_s(r,t)/\partial t = \tau_s C_s(r,t)\,\varphi(r) \quad \text{(B2)}$$

Substituting Eq. (B1) in Eq. (B2) and integrating over time leads to the concentration distribution:

$$C_s(r,t) = C_{so}\exp[-\tau_s K_s \varphi(r) t] \quad \text{(B3)}$$

where C_{so} (μg g^{-1}) is the initial drug concentration. According to Eq. (B3), the drug concentration decreases exponentially in time with a complex spatial dependence that depends on the light distribution. The effect of photobleaching on light absorption is calculated by substituting Eq. (B3) in Eq. (B2) and integrating over time:

$$W_s(r,t) = (C_{so}/K_s)\{1-\exp[-\tau_s K_s \varphi(r) t]\} \quad \text{(B4)}$$

Eq. (B4) indicates that the maximum absorbed energy density W_s after a lengthy irradiation equals C_{so}/K_s. Tissue necrosis requires $W_s \geq W_s^*$. The subsequent analysis is carried out for FS delivery. The essential conclusions should be the same for other light delivery modes. Substituting Eq. (A3) in Eq. (B2) and evaluating at the necrosis threshold leads to:

$$d_n = \delta \log_e\left\{\frac{-K_s\tau_s M(E_o t)}{\log_e(1-K_s W_s^*/C_{so})}\right\} \quad \text{(B5)}$$

Comparing Eqs. (B5) and (A8) shows that photobleaching reduces the necrosis depth by $\delta \log_e[-\log_e(1-x)/x]$, where $x \equiv K_s W_s^*/C_{so} = K_s\tau_s q^*$.

K_s may be calculated from clinical results indicating that PDT of BCC with PF requires about 30 J cm^{-2} at standard conditions (2.0 mg kg^{-1}) and about 200 J cm^{-2} at 1.0 mg kg^{-1} [21]. Since W_s^* does not depend on the drug dose, these values of C_{so} and (E_ot) can be substituted in Eq. (B5) and the results equated:

$$\frac{(E_o t)'}{E_o t} = \frac{\log_e[1-(C_{so}/C_{so}')x]}{\log_e(1-x)} \quad \text{(B6)}$$

where the primed values apply to the lower drug dose. The numerical solution of Eq. (B6) leads to $x = 0.495$. Taking $\tau_s = 0.005$ μg^{-1} g cm^{-1} for PF in tumor tissue at 630 nm [29] and $q^* = 39$ J cm^{-2} leads to $K_s = 2.54$ μg g^{-1} J^{-1} cm^3. The corresponding rate constant in terms of the incident dose is $\approx K_s\tau_s M/e = 0.025$ J^{-1} cm^2). Substituting x in Eq. (B5) for PF at standard conditions shows that photobleaching reduces d_n by 0.32δ at any light dose.

The present analysis of drug elimination follows the approach in Ref. [13] in which it was assumed that photobleaching and elimination obey first-order kinetics. The modified form of Eq. (B3) is

$$C_s(r,t) = C_{so}\exp[-\tau_s K_s \varphi(r) t - \beta t] \quad \text{(B7)}$$

where β is the drug elimination rate constant and $T = \log_e 2/\beta$. Substituting Eq. (B7) in Eq. (B2) and integrating over time gives

$$W_s(r,t) = \frac{\tau_s C_{so} \varphi(r)}{\tau_s K_s \varphi(r) + \beta} \{1 - \exp[-\tau_s K_s \varphi(r) t - \beta t]\} \quad \text{(B8)}$$

Eq. (B8) reduces to the corresponding expressions for negligible elimination or negligible photobleaching for $\beta = 0$ and $K_s = 0$, respectively. The necrosis condition for FS delivery is

$$\frac{A(E_o t)}{\tau_s K_s (E_o t) + \beta t} \{1 - \exp[-(\tau_s K_s E_o + \beta)]t\} = q^* \quad \text{(B9)}$$

where $A \equiv M \exp(-d_n/\delta)$. Elimination differs from photobleaching because d_n depends on the incident irradiance E_o as well as the incident fluence $(E_o t)$.

Photobleaching protects normal tissues with low initial drug concentrations. The maximum necrosis depth that can be achieved in tumor tissue without necrosis of normal tissue (d_n^*) can be calculated with Eq. (B5) by assuming the same values of $(E_o t)$, τ_s, K_s, and M in the normal and tumor tissues:

$$\exp(-d_n^*/\delta) = \log_e\{1 - (C_{so}'/C_{so})[1 - \exp(y)]\}/y \quad \text{(B10)}$$

where $y \equiv \tau_s K_s M(E_o t)$. Some comparisons of Eqs. (B10) and (B5) in Section 4.2 show that $d_n^* > d_n$ for PF at standard conditions.

References

[1] L.I. Grossweiner, Optical dosimetry in photodynamic therapy, Lasers Surg. Med. 6 (1986) 462–466.

[2] T.S. Mang, T.J. Dougherty, W.R. Potter, D.G. Boyle, S. Sommer, J. Moan, Photobleaching of porphyrins used for photodynamic therapy and implications for therapy, Photochem. Photobiol. 45 (1987) 501–506.

[3] A.E. Profio, D.R. Doiron, Transport of light in tissue in photodynamic therapy, Photochem. Photobiol. 46 (1987) 591–599.

[4] L.I. Grossweiner, J.H. Hill, R.V. Lobraico, Photodynamic therapy of head and neck squamous cell carcinoma: Optical dosimetry and clinical trial, Photochem. Photobiol. 46 (1987) 911–917.

[5] A.E. Profio, D.R. Doiron, Dose measurements in photodynamic therapy of cancer, Lasers Surg. Med. 7 (1987) 1–5.

[6] L.I. Grossweiner, Optical dosimetry in photodynamic therapy, in: R.H. Douglas, J. Moan, F. Dall'Acqua (Eds.), Light in Biology and Medicine, vol. 1, Plenum, New York, 1988, pp. 61–66.

[7] S.L. Jacques, Simple theory, measurements, and rules of thumb for dosimetry during photodynamic therapy, Proc. Soc. Photo Opt. Instr. Eng. 1065 (1989) 100–108.

[8] L.I. Grossweiner, B.L. Wenig, R.V. Lobraico, Treatment planning and clinical trials on head and neck carcinoma, Proc. Soc. Photo Opt. Instr. Eng. 1203 (1990) 53–61.

[9] L.I. Grossweiner, Optical dosimetry in photodynamic therapy, in: D. Kessel (Ed.), Photodynamic Therapy of Neoplastic Disease, vol. I, CRC Press, Boca Raton, FL, 1990, pp. 91–108.

[10] B.C. Wilson, M.S. Patterson, The determination of light fluence distributions in photodynamic therapy, in: D. Kessel (Ed.), Photodynamic Therapy of Neoplastic Disease, vol. I, CRC Press, Boca Raton, FL, 1990, pp.129–145.

[11] M.S. Patterson, J.D. Mouton, B.C. Wilson, B. Chance, Applications of time-resolved measurements to photodynamic therapy dosimetry, Proc. Soc. Photo Opt. Instr. Eng. 1203 (1990) 62–75.

[12] L.I. Grossweiner, Light dosimetry model for photodynamic therapy treatment planning, Lasers Surg. Med. 11 (1991) 165–173.

[13] L.O. Svaasand, W.R. Potter, The implications of photobleaching for photodynamic therapy, in: B.W. Henderson, T.J. Dougherty (Eds.), Photodynamic Therapy, Marcel Dekker, New York, 1992, pp. 369–385.

[14] W.M. Star, B.C. Wilson, M.S. Patterson, Light delivery and optical dosimetry in photodynamic therapy of solid tumors, in: B.W. Henderson, T.J. Dougherty (Eds.), Photodynamic Therapy, Marcel Dekker, New York, 1992, pp. 335–368.

[15] L.I. Grossweiner, The Science of Phototherapy, CRC Press, Boca Raton, FL, 1994.

[16] W.-F. Cheong, S.A. Prahl,, A.W. Welch, A review of the optical properties of biological tissues, IEEE J. Quant. Elect. 26 (1990) 2166–2185.

[17] S.L. Marcus, Clinical photodynamic therapy: The continuing evolution, in: B.W. Henderson, T.J. Dougherty (Eds.), Photodynamic Therapy, Marcel Dekker, New York, 1992, pp. 219–268.

[18] H.J. van Staveren, J.F. Beck, J.W.H. Ramaekers, M. Keijzer, W.M. Star, Integrating sphere effect in whole bladder wall photodynamic therapy: I. 532 nm versus 630 nm optical radiation, Phys. Med Biol. 39 (1994) 947–959.

[19] C.M. Gardner, S.L. Jacques, A.J. Welch, Light transport in tissue: Accurate expressions for one-dimensional fluence rate and escape function based upon Monte Carlo simulation, Lasers Surg. Med. 18 (1996) 129–138.

[20] L.R. Jones, L.I. Grossweiner, Singlet oxygen generation by Photofrin in homogeneous and light-scattering media, J. Photochem. Photobiol. B: Biol. 26 (1994) 249–256.

[21] B.W. Wilson, T.S. Mang, M.C. Cooper, H. Stoll, Use of photodynamic therapy for the treatment of extensive basal cell carcinoma, Facial Plastic Surg. 6 (1990) 185–189.

[22] G.M. Vincent, J. Fox, G. Charlton, J.S. Hill, R. McClane, J.D. Spikes, Presence of blood significantly decreases transmission of 630 nm laser light, Lasers Surg. Med. 11 (1991) 399–403.

[23] R.C. Hillegersberg, J.W. Pickering, M. Asiders, J.F. Beek, Optical properties of rat liver and tumor at 633 nm: Photofrin enhances scattering, Lasers Surg. Med. 13 (1993) 31–39.

[24] L.R. Jones, L.I. Grossweiner, Effects of Photofrin on in vivo skin reflectivity, J. Photochem. Photobiol. B: Biol. 33 (1996) 153–156.

[25] L.I. Grossweiner, L.R. Jones, I.K. Koehler, M.D. Bilgin, Effect of Photofrin (Reg. tM) on skin reflection of basal cell nevus syndrome patients, Soc. Photo Opt. Instr. Eng. 2675 (1996) 2–12.

[26] B.L. Wenig, D.M. Kurtzman, L.I. Grossweiner, M.G. Mafee, D. Harris, R.V. Lobraico, R.A. Prycz, E.L. Appelbaum, Photodynamic therapy in the treatment of squamous cell squamous cell carcinoma of the head and neck, Arch. Otolaryngol. Head Neck Surg. 116 (1990) 1267–1270.

[27] L.I. Grossweiner, A.A. Al-Karmi, P.W. Johnson, K.R. Brader, Modeling tissue heating with a pulsed Nd:YAG laser, Lasers Surg. Med. 10 (1990) 295–302.

[28] L.O. Svaasand, R. Ellingsen, Optical properties of human brain, Photochem. Photobiol. 38 (1983) 293–299.

[29] A.E. Profio, L.R. Wudl, J. Sarnaik, Dosimetry methods in photoradiation therapy, in: D. Kessel (Eds.), Methods in Porphyrin Photosensitization, Plenum, New York, 1985, pp. 35–41.

[30] G. Yoon, Absorption and scattering of laser light in biological media—Mathematical modeling and methods for determining optical properties, Ph.D. Dissertation, Univ. Texas at Austin, 1988.

[31] R. Splinter, W.F. Cheong, M.J.C. van Gemert, A.J. Welch, In vitro optical properties of human and canine brain and urinary bladder tissues at 633 nm, Lasers Surg. Med. 9 (1989) 37–41.

[32] R. Marchesini, A. Bertoni, A. Andeola, E. Melloni, A.E. Sichirolio, Extinction and absorption coefficients and scattering phase functions of human tissues in vitro, Appl. Opt. 28 (1989) 2318–2324.

[33] S.L. Jacques, C.A. Alter, S.A. Prahl, Angular dependence of HeNe laser light scattering by human dermis, Lasers Life Sci. 4 (1987) 309–333.

[34] R. Marchesini, C. Clemente, E. Pignoli, M. Brambilla, Optical properties of in vitro epidermis and their possible relationship with optical properties of in vivo skin, J. Photochem. Photobiol. B: Biol. 16 (1992) 127–140.

[35] S. Andreola, A. Bertoni, R. Marchesini, E. Melloni, Evaluation of optical characteristics of different human tissues, Lasers Surg. Med. 8 (1988) 142 (abstract).